ELSEVIER

An immersed boundary method for interfacial flows with insoluble surfactant

Ming-Chih Lai [a,*], Yu-Hau Tseng [a], Huaxiong Huang [b]

[a] *Department of Applied Mathematics, National Chiao Tung University, 1001, Ta Hsueh Road, Hsinchu 300, Taiwan*
[b] *Department of Mathematics and Statistics, York University, Toronto, Ontario, Canada M3J 1P3*

Abstract

In this paper, an immersed boundary method is proposed for the simulation of two-dimensional fluid interfaces with insoluble surfactant. The governing equations are written in a usual immersed boundary formulation where a mixture of Eulerian flow and Lagrangian interfacial variables are used and the linkage between these two set of variables is provided by the Dirac delta function. The immersed boundary force comes from the surface tension which is affected by the distribution of surfactant along the interface. By tracking the interface in a Lagrangian manner, a simplified surfactant transport equation is derived. The numerical method involves solving the Navier–Stokes equations on a staggered grid by a semi-implicit pressure increment projection method where the immersed interfacial forces are calculated at the beginning of each time step. Once the velocity value and interfacial configurations are obtained, surfactant concentration is updated using the transport equation. In this paper, a new symmetric discretization for the surfactant concentration equation is proposed that ensures the surfactant mass conservation numerically. The effect of surfactant on drop deformation in a shear flow is investigated in detail.
© 2008 Elsevier Inc. All rights reserved.

Keywords: Immersed boundary method; Interfacial flow; Navier–Stokes equations; Surfactant

1. Introduction

In this paper, we propose an immersed boundary method for the simulation of two-dimensional fluid interfaces with insoluble surfactant. Surfactant are surface active agents that adhere to the fluid interface and affect the interface surface tension. Surfactant play an important role in many applications in the industries of food, cosmetics, oil, etc. For instance, the daily extraction of ore rely on the subtle effects introduced by the presence of surfactant [5]. In a liquid–liquid system, surfactant allow small droplets to be formed and used as an emulsion. Surfactant also play an important role in water purification and other applications where micro-sized bubbles are generated by lowering the surface tension of the liquid–gas interface. In microsystems with the

---

* Corresponding author. Tel.: +886 3 5731361; fax: +886 3 5724679.
E-mail addresses: mclai@math.nctu.edu.tw (M.-C. Lai), yhtseng@math.nctu.edu.tw (Y.-H. Tseng), hhuang@yorku.ca (H. Huang).

presence of interfaces, it is extremely important to consider the effect of surfactant since in such cases the capillary effect dominates the inertia of the fluids [20].

The immersed boundary (IB) method proposed by Peskin [14], has been applied successfully to blood–valve interaction and other biological problems. The IB formulation employs a mixture of Eulerian and Lagrangian variables, where the immersed boundary is represented by a set of discrete Lagrangian markers embedding in the Eulerian fluid domain. Those markers can be treated as force generators to the fluid while being carried by the fluid motion. The interaction between the Lagrangian force generators (markers) and the fluid motion, described by variables defined on the fixed Eulerian grid, is linked by a properly chosen discretized delta function. Most IB applications in the literature belong to the fluid–structure problems, and they can be found in a recent review of Peskin [15]. However, there is comparatively less work on the application of the IB method to viscous, incompressible multi-phase flow problems. Perhaps the most successful one is the front-tracking method proposed by Tryggvason et al. [21,22] which uses an approach similar to the immersed boundary method.

In the case of interfacial flows with surfactant, Ceniceros [4] used a hybrid level set and front tracking approach to study the effects of surfactant on the formation of capillary waves. Lee and Pozrikids [12] used Peskin's immersed boundary idea to study the effects of surfactant on the deformation of drops and bubbles in Navier–Stokes flows. The surfactant convection–diffusion equation in these papers is based on the formulation proposed by Wong et al. [23], and the conservation of total mass of surfactant on the interface has not been rigorously investigated numerically.

James and Lowengrub [9] have proposed a surfactant-conserving volume-of-fluid method for interfacial flows with insoluble surfactant. Instead of solving the surfactant concentration equation based on Stone's derivation [19] directly, the authors relate the surfactant concentration to the ratio of the surfactant mass and surface area so that they are tracked independently. The method has been applied to study the axis-symmetric drop deformation in extensional flows. Recently, Xu et al. [25] develop a level-set method for interfacial Stokes flows with surfactant. Their method couples surfactant transport, solved in an Eulerian domain [26] with Stokes flow field, solved by the immersed interface method [11] with jump conditions across the interface. However, the method does not conserve the mass automatically and numerical scaling is used to enforce the conservation of surfactant on the interface numerically. Recently, Muradoglu and Tryggvason [13] have proposed a front-tracking method for computation of interfacial flows with soluble surfactant. They consider the axis-symmetric motion and deformation of a viscous drop moving in a circular tube.

In this paper, we propose an immersed boundary method to simulate the interfacial problems with insoluble surfactant. By tracking the interface in a Lagrangian manner, the surfactant concentration equation becomes much simpler than the one in [23]. Our numerical method involves solving the Navier–Stokes equations on a staggered grid by a semi-implicit pressure increment projection method where the immersed interfacial forces are calculated at the beginning of each time step. A new symmetric discretization for the surfactant concentration equation is proposed so that the total mass of surfactant is conserved numerically. The effect of surfactant on drop deformation in a shear flow is then investigated in detail.

The rest of the paper is organized as follows. In Section 2, we present the governing equations which includes the immersed boundary formulation and the surfactant concentration equation in Lagrangian coordinates on the interface. The numerical method is described in Section 3 which includes an algorithm of solving the Navier–Stokes equations and a conservative scheme for the surfactant equation. The effect of surfactant on drop deformation in a shear flow is investigated numerically in Section 4. Some concluding remarks and brief discussion on future directions are given in Section 5.

2. The governing equations

Consider an incompressible two-phase flow problem consisting of fluids 1 and 2 in a fixed two-dimensional square domain $\Omega = [a, b] \times [c, d] = \Omega_1 \cup \Omega_2$ where an interface Σ separates Ω_1 from Ω_2. Here, we assume the interface is a simple closed curve immersed in the fluid domain, and is contaminated by the surfactant so that the distribution of the surfactant changes the surface tension accordingly. In each fluid region, the Navier–Stokes equations are satisfied as

$$\rho_i\left(\frac{\partial \mathbf{u}_i}{\partial t} + (\mathbf{u}_i \cdot \nabla)\mathbf{u}_i\right) = \nabla \cdot \mathbf{T}_i + \rho_i\mathbf{g}, \quad \text{in } \Omega_i, \tag{1}$$

$$\nabla \cdot \mathbf{u}_i = 0, \quad \text{in } \Omega_i, \tag{2}$$

$$\boldsymbol{u} = \boldsymbol{u}_{\mathrm{b}}, \quad \text{in } \partial\Omega, \tag{3}$$

where for $i = 1, 2$ in each fluid domain, $\mathbf{T}_i = -p_i\mathbf{I} + \mu_i(\nabla\mathbf{u}_i + \nabla\mathbf{u}_i^{\mathrm{T}})$ is the stress tensor, p_i is the pressure, $\mathbf{u}_i$ is the fluid velocity, ρ_i is the density, μ_i is the viscosity, and $\mathbf{g}$ is the gravitational constant.

It is well-known that, across the interface Σ, the velocity is continuous

$$[\mathbf{u}]_\Sigma = \mathbf{u}|_{\Sigma,2} - \mathbf{u}|_{\Sigma,1} = 0 \tag{4}$$

and the normal stress jump is balanced by the interfacial force $\mathbf{F}$ (defined only on Σ) as

$$[\mathbf{Tn}]_\Sigma + \mathbf{F} = 0, \tag{5}$$

where $\mathbf{n}$ is the unit normal vector on Σ directed towards fluid 2. Since it is not easy to solve the Navier–Stokes equations (1) and (2) in Ω with jump conditions (4) and (5) on Σ, especially when the interface is moving. In order to formulate the problem using the immersed boundary approach, we simply treat the interface as an immersed boundary that exerts force $\mathbf{F}$ to the fluids and moves with local fluid velocity. In this paper, we consider the case of equal viscosity $\mu_1 = \mu_2 = \mu$, equal density $\rho_1 = \rho_2 = \rho$, and neglect gravity. However, the current formulation can be extended straightforwardly to general two phase flow with different density and viscosity. The present interfacial force term in delta function formulation and the surfactant concentration equation are the same as the single phase problem. The major difference comes from the Navier–Stokes formulation and their numerics.

2.1. Immersed boundary formulation

Throughout this paper, the interface Σ is represented by a parametric form $(X(s,t), Y(s,t)), 0 \leqslant s \leqslant L_{\mathrm{b}}$, where s is the parameter of the initial configuration of the interface, which is not necessarily the arc-length.

Using the non-dimensionalization process [9,25], we can write down our governing equations in the usual immersed boundary formulation as follows.

$$\frac{\partial \mathbf{u}}{\partial t} + (\mathbf{u} \cdot \nabla)\mathbf{u} + \nabla p = \frac{1}{Re}\nabla^2\mathbf{u} + \frac{1}{ReCa}\mathbf{f}, \tag{6}$$

$$\nabla \cdot \mathbf{u} = 0, \tag{7}$$

$$\mathbf{f}(\mathbf{x},t) = \int_\Sigma \mathbf{F}(s,t)\delta(\mathbf{x} - \mathbf{X}(s,t))\,\mathrm{d}s, \tag{8}$$

$$\frac{\partial \mathbf{X}(s,t)}{\partial t} = \mathbf{u}(\mathbf{X}(s,t),t) = \int_\Omega \mathbf{u}(\mathbf{x},t)\delta(\mathbf{x} - \mathbf{X}(s,t))\,\mathrm{d}\mathbf{x}, \tag{9}$$

$$\mathbf{F}(s,t) = \frac{\partial}{\partial s}(\sigma(s,t)\boldsymbol{\tau}(s,t)), \tag{10}$$

$$\boldsymbol{\tau}(s,t) = \frac{\frac{\partial \mathbf{X}}{\partial s}}{\left|\frac{\partial \mathbf{X}}{\partial s}\right|}. \tag{11}$$

The dimensionless numbers are the Reynolds number (Re) describing the ratio between the inertial force and the viscous force, and the capillary number (Ca) describing the strength of the surface tension. Eqs. (8) and (9) represent the interaction between the immersed interface and the fluids. In particular, Eq. (8) describes the force ($\mathbf{f}$) acting on the fluid due to the interfacial force ($\mathbf{F}$), which is defined only on the interface and must be balanced by the normal stress as shown in Eq. (5). Here, σ is the surface tension, and $\boldsymbol{\tau}$ is the unit tangent vector on the interface. Eq. (9) states that the interface moves with the fluid velocity which is consistent with (4). The present formulation employs a mixture of Eulerian ($\mathbf{x}$) and Lagrangian ($\mathbf{X}$) variables which are linked by the two-dimensional Dirac delta function $\delta(\mathbf{x}) = \delta(x)\delta(y)$.

The interfacial force **F** arises from the surface tension and its form is derived from Laplace–Young condition [10]. One can further take derivatives explicitly so that

$$\mathbf{F}(s,t) = \frac{\partial}{\partial s}(\sigma\boldsymbol{\tau}) = \frac{\partial\sigma}{\partial s}\boldsymbol{\tau} + \sigma\frac{\partial\boldsymbol{\tau}}{\partial s} = \frac{\partial\sigma}{\partial s}\boldsymbol{\tau} + \sigma\kappa\boldsymbol{n}\left|\frac{\partial\mathbf{X}}{\partial s}\right|, \tag{12}$$

where κ is the curvature of the interface and $\boldsymbol{n}$ is the unit outward normal. The first term on the right-hand side of Eq. (12) is the Marangoni force (the tangential force) and the second one is the capillary force (the normal force). (Note that, we have different sign convention in the capillary term since the sign of curvature is different from that in the literature [8,9,12,25]. For circular interface, the present curvature is negative.) Note also that if the surface tension is a constant, then the force only exerts in the normal direction. However, when the interface is contaminated by the surfactant, the distribution of the surfactant changes the surface tension accordingly. Generally speaking, the higher the surfactant concentration, the less the surface tension. The relation between surface tension and surfactant concentration can be described by the Langmuir equation of state [17]. As in [4], the following linear approximation of Langmuir equation is used

$$\sigma(\Gamma) = \sigma_c(1 - \beta\Gamma), \tag{13}$$

where Γ is the surfactant concentration, σ_c is the surface tension of a clean interface, and β satisfying $0 \leqslant \beta < 1$ is a dimensionless number that measures the sensitivity of surface tension to changes in surfactant concentration.

In order to close the system, we still need one more equation for surfactant concentration evolution. As mentioned before, surfactant are insoluble to the buck fluids so they are simply convected and diffused along the interface. Since there is no exchange between the interface and the bulk fluids, the total mass of the surfactant must be conserved. The equation of surfactant concentration is derived in next subsection.

2.2. Surfactant concentration equation

The basic equation for surfactant transport equation along a deforming interface has been derived by Scriven [18], Aris [2], and Waxman [24]. All three papers derived the surfactant equation relying heavily on differential geometry. Stone [19], however, presented a simple derivation of the time-dependent convective–diffusion equation for surfactant transport along a deforming interface. In this subsection, we present a slightly different derivation from Stone for the surfactant transport equation which will be used as one of our governing equations for numerical computation. Our derivation is in the same spirit of the immersed boundary approach. A more detailed derivation for surfactant concentration equation along a two-dimensional parametric deforming surface in three-dimensional fluid domains can be found in our recent work [7].

Let $L(t)$ be an interfacial segment where the surfactant concentration (the mass of the surfactant per unit length) is defined. Since the surfactant remain on the material element and do not transport or diffuse to the surrounding bulk fluids, the mass on the segment is conserved

$$\frac{\mathrm{d}}{\mathrm{d}t}\int_{L(t)} \Gamma(l,t)\,\mathrm{d}l = 0, \tag{14}$$

where $\mathrm{d}l$ is the arc-length element. To apply the time derivative more easily, we rewrite the above equation in terms of the initial parameter s as

$$\frac{\mathrm{d}}{\mathrm{d}t}\int_{L(0)} \Gamma(s,t)\left|\frac{\partial\mathbf{X}}{\partial s}\right|\mathrm{d}s = 0. \tag{15}$$

By taking the time derivative inside the integral, we obtain

$$\int_{L(0)} \left(\frac{\partial\Gamma}{\partial t}\left|\frac{\partial\mathbf{X}}{\partial s}\right| + \Gamma\frac{\partial}{\partial t}\left|\frac{\partial\mathbf{X}}{\partial s}\right|\right)\mathrm{d}s = 0. \tag{16}$$

Note that, in our present formulation, both the interface and surfactant concentration are tracked in a Lagrangian manner. Thus, the time derivative of the first term in Eq. (16) is exactly the material derivative

of Stone's derivation [19]. The time derivative of the second term is due to interface stretching. Now we need to compute the rate of the stretching factor, and using Eq. (9), we have

$$\frac{\partial}{\partial t}\left|\frac{\partial \mathbf{X}}{\partial s}\right| = \frac{\frac{\partial X}{\partial s}\frac{\partial}{\partial s}\left(\frac{\partial X}{\partial t}\right) + \frac{\partial Y}{\partial s}\frac{\partial}{\partial s}\left(\frac{\partial Y}{\partial t}\right)}{\left|\frac{\partial \mathbf{X}}{\partial s}\right|} = \frac{\frac{\partial X}{\partial s}\frac{\partial u}{\partial s} + \frac{\partial Y}{\partial s}\frac{\partial v}{\partial s}}{\left|\frac{\partial \mathbf{X}}{\partial s}\right|} = \frac{\frac{\partial X}{\partial s}\left(\nabla u \cdot \frac{\partial \mathbf{X}}{\partial s}\right) + \frac{\partial Y}{\partial s}\left(\nabla v \cdot \frac{\partial \mathbf{X}}{\partial s}\right)}{\left|\frac{\partial \mathbf{X}}{\partial s}\right|} = \left(\frac{\partial \mathbf{u}}{\partial \boldsymbol{\tau}} \cdot \boldsymbol{\tau}\right)\left|\frac{\partial \mathbf{X}}{\partial s}\right|$$

$$= (\nabla_s \cdot u)\left|\frac{\partial \mathbf{X}}{\partial s}\right|. \tag{17}$$

Here, the notation $\nabla_s \cdot u$ means the surface divergence which is used commonly in the literature. Since the material segment is arbitrary, we thus have

$$\frac{\partial \Gamma}{\partial t} + (\nabla_s \cdot \boldsymbol{u})\Gamma = 0. \tag{18}$$

If we allow surfactant diffusion along the interface, we obtain the surfactant transport-diffusion equation as

$$\frac{\partial \Gamma}{\partial t} + (\nabla_s \cdot \boldsymbol{u})\Gamma = \frac{1}{Pe_s}\frac{\partial}{\partial s}\left(\frac{\partial \Gamma}{\partial s}\bigg/\left|\frac{\partial \mathbf{X}}{\partial s}\right|\right)\bigg/\left|\frac{\partial \mathbf{X}}{\partial s}\right|, \tag{19}$$

where Pe_s is the surface Peclet number [9]. We note that surface diffusion is also written in terms of initial parameter s.

Let us summarize this section by pointing out the differences and similarities between our present surfactant equation (19) and the ones derived in the literature [19,23]. As we discussed before, the present time derivative is exactly the material derivative with the material parameter s fixed, while the time derivative used in [19] is keeping the material coordinates $\mathbf{X}$ fixed. Wong et al. [23] argued that the time derivative term in Stone's surfactant equation causes ambiguity in numerical discretization since the material coordinates is time-dependent as well. Wong et al. [23] provide an alternative derivation for the surfactant equation, where the concentration time derivative is applied by keeping the material parameter s fixed. This is exactly what we have done here. It is interesting (but not surprising) to conclude that the surfactant concentration equation in [23] can be simplified to our present form (19) by substituting Eq. (9) into their equation.

3. Numerical method

In this paper, the fluid flow variables are defined on a staggered marker-and-cell (MAC) mesh introduced by Harlow and Welsh [6]; that is, the pressure is defined on the grid points labelled as $\mathbf{x} = (x_i, y_j) = ((i - 1/2)h, (j - 1/2)h)$ for $i, j = 1, 2 \ldots, N$, the velocity components u and v are defined at $(x_{i-1/2}, y_j) = ((i - 1)h, (j - 1/2)h)$ and $(x_i, y_{j-1/2}) = ((i - 1/2)h, (j - 1)h)$, respectively, where the spacing $h = \Delta x = \Delta y$. For the immersed interface, we use a collection of discrete points $s_k = k\Delta s, k = 0, 1, \ldots M$ such that the Lagrangian markers are denoted by $\mathbf{X}_k = \mathbf{X}(s_k) = (X_k, Y_k)$. The surfactant concentration Γ_k, surface tension σ_k are defined at the "half-integer" points given by $s_{k+1/2} = (k + 1/2)\Delta s$. Without loss of generality, for any function defined on the interface $\phi(s)$, we approximate the partial derivative $\frac{\partial \phi}{\partial s}$ by

$$D_s\phi(s) = \frac{\phi(s + \Delta s/2) - \phi(s - \Delta s/2)}{\Delta s}. \tag{20}$$

By using this finite difference convention, the interface stretching factor can be approximated by $|D_s X_k|$, and thus the unit tangent vector $\boldsymbol{\tau}_k$ are also defined at the "half-integer" points.

Let Δt be the time step size, and n be the superscript time step index. At the beginning of each time step, e.g., step n, the variables $\mathbf{X}_k^n = \mathbf{X}(s_k, n\Delta t)$, $\Gamma_k^n = \Gamma(s_{k+1/2}, n\Delta t)$, $\mathbf{u}^n = \mathbf{u}(\mathbf{x}, n\Delta t)$, and $p^{n-1/2} = p(\mathbf{x}, (n - 1/2)\Delta t)$ are all given. The details of the numerical time integration are as follows.

1. Compute the surface tension and unit tangent on the interface as

$$\sigma_k^n = \sigma_c(1 - \beta\Gamma_k^n), \tag{21}$$

$$\boldsymbol{\tau}_k^n = \frac{D_s X_k^n}{|D_s X_k^n|}, \tag{22}$$

both of which hold for $s_{k+1/2} = (k + 1/2)\Delta s$. Then we define the interface force as

$$\boldsymbol{F}_k^n = D_s(\sigma_k^n \boldsymbol{\tau}_k^n),$$ (23)

at point $\mathbf{X}_k$.

2. Distribute the force from the markers to the fluid by

$$\boldsymbol{f}^n(x) = \sum_k \boldsymbol{F}_k^n \delta_h(\boldsymbol{x} - \boldsymbol{X}_k^n)\Delta s,$$ (24)

where the smooth version of Dirac delta function in [15] is used.

3. Solve the Navier–Stokes equations. This can be done by the following second-order accurate projection method [3], where the nonlinear term is approximated by the Adams–Bashforth scheme and the viscous term is approximated by the Crank–Nicholson scheme.

$$(\boldsymbol{u} \cdot \nabla_h)\mathbf{u}^{n+1/2} = \frac{3}{2}(\boldsymbol{u}^n \cdot \nabla_h)\mathbf{u}^n - \frac{1}{2}(\boldsymbol{u}^{n-1} \cdot \nabla_h)\mathbf{u}^{n-1},$$ (25)

$$\frac{\mathbf{u}^* - \mathbf{u}^n}{\Delta t} + (\boldsymbol{u} \cdot \nabla_h)\mathbf{u}^{n+1/2} = -\nabla p^{n-1/2} + \frac{1}{2Re}\nabla_h^2(\mathbf{u}^* + \mathbf{u}^n) + \frac{\mathbf{f}^n}{ReCa},$$ (26)

$$\boldsymbol{u}^* = \boldsymbol{u}_b, \quad \text{on } \partial\Omega,$$ (27)

$$\nabla_h^2 \phi^{n+1} = \frac{\nabla_h \cdot \boldsymbol{u}^*}{\Delta t}, \quad \frac{\partial \phi}{\partial n} = 0, \quad \text{on } \partial\Omega,$$ (28)

$$\boldsymbol{u}^{n+1} = \boldsymbol{u}^* - \Delta t \nabla_h \phi^{n+1},$$ (29)

$$p^{n+1/2} = p^{n-1/2} + \phi^{n+1} - \frac{\nabla_h \cdot \boldsymbol{u}^*}{2Re}.$$ (30)

Here ∇_h is the standard centered difference operator on the staggered grid. One can see that the above Navier–Stokes solver involves solving two Helmholtz equations for velocity u^* and one Poisson equation for pressure. These elliptic equations are solved using the fast Poisson solver provided by the public software package Fishpack [1].

4. Interpolate the new velocity on the fluid lattice points onto the marker points and move the marker points to new positions.

$$\boldsymbol{U}_k^{n+1} = \sum_x \boldsymbol{u}^{n+1} \delta_h(\boldsymbol{x} - \boldsymbol{X}_k^n)h^2,$$ (31)

$$\boldsymbol{X}_k^{n+1} = \boldsymbol{X}_k^n + \Delta t \boldsymbol{U}_k^{n+1}.$$ (32)

5. Update surfactant concentration distribution Γ_k^{n+1}. Since the surfactant is insoluble, the total mass on the interface must be conserved. Thus, it is important to develop a numerical scheme for the surfactant concentration equation to preserve the total mass. This can be done as follows.

Firstly, let us rewrite the surfactant concentration equation (19) by multiplying the stretching factor on the both sides of the equation as

$$\frac{\partial\Gamma}{\partial t}\left|\frac{\partial\mathbf{X}}{\partial s}\right| + (\nabla_s \cdot \boldsymbol{u})\left|\frac{\partial\mathbf{X}}{\partial s}\right|\Gamma = \frac{1}{Pe_s}\frac{\partial}{\partial s}\left(\frac{\partial\Gamma}{\partial s}\bigg/\left|\frac{\partial\mathbf{X}}{\partial s}\right|\right).$$ (33)

Then substitute Eq. (17) of rate of stretching factor into the above equation, we have

$$\frac{\partial\Gamma}{\partial t}\left|\frac{\partial\mathbf{X}}{\partial s}\right| + \frac{\partial}{\partial t}\left|\frac{\partial\mathbf{X}}{\partial s}\right|\Gamma = \frac{1}{Pe_s}\frac{\partial}{\partial s}\left(\frac{\partial\Gamma}{\partial s}\bigg/\left|\frac{\partial\mathbf{X}}{\partial s}\right|\right).$$ (34)

Now we discretize the above equation by the Crank–Nicholson scheme in a symmetric way as

$$\frac{\Gamma_k^{n+1} - \Gamma_k^n}{\Delta t} \frac{|D_s X_k^{n+1}| + |D_s X_k^n|}{2} + \frac{|D_s X_k^{n+1}| - |D_s X_k^n|}{\Delta t} \frac{\Gamma_k^{n+1} + \Gamma_k^n}{2}$$

$$= \frac{1}{2Pe_s} \frac{1}{\Delta s} \left(\frac{(\Gamma_{k+1}^{n+1} - \Gamma_k^{n+1})/\Delta s}{(|D_s X_{k+1}^{n+1}| + |D_s X_k^{n+1}|)/2} - \frac{(\Gamma_k^{n+1} - \Gamma_{k-1}^{n+1})/\Delta s}{(|D_s X_k^{n+1}| + |D_s X_{k-1}^{n+1}|)/2} \right) + \frac{1}{2Pe_s}$$

$$\times \frac{1}{\Delta s} \left(\frac{(\Gamma_{k+1}^n - \Gamma_k^n)/\Delta s}{(|D_s X_{k+1}^n| + |D_s X_k^n|)/2} - \frac{(\Gamma_k^n - \Gamma_{k-1}^n)/\Delta s}{(|D_s X_k^n| + |D_s X_{k-1}^n|)/2} \right). \tag{35}$$

Since the new interface marker location X_k^{n+1} is obtained in the previous step, the above discretization results in a symmetric tri-diagonal linear system which can be solved easily. More importantly, the total mass of surfactant is conserved numerically; that is,

$$\sum_k \Gamma_k^{n+1} |D_s X_k^{n+1}| \Delta s = \sum_k \Gamma_k^n |D_s X_k^n| \Delta s. \tag{36}$$

(Note that, the summation is exactly the mid-point rule discretization for the integral in Eq. (15).) The above equality can be easily derived by taking the summation of both sides of Eq. (35) and using the periodicity of those quantities.

4. Numerical results

The effect of surfactant on the deformation of a drop is of considerable interest in polymer and emulsion industries. It is also a good theoretical model for illustrating subtle physics in viscous interfacial flow. In this section, the immersed boundary method is applied to study the effect of surfactant on drop deformation in Navier–Stokes flows.

Following the set up in [25], we consider a computational domain $\Omega = [-5, 5] \times [-2, 2]$ where a circular drop of radius one is initially located at the center of the domain. We apply a steady shear flow to the drop; that is, we set the boundary condition $u_b = (0.5y, 0)$, for $-2 \leqslant y \leqslant 2$. For comparison purposes, both clean (without surfactant) and contaminated (with surfactant) drops are used in these computations. Using the equation of state given by Eq. (13), $\beta = 0$ implies no contamination, in which case we do not need to solve the surfactant equation (19). Throughout this paper, we set $\sigma_c = 1$ so the clean interface has a uniform surface tension $\sigma = \sigma_c$. For the contaminated case, the initial surfactant concentration is uniformly distributed along the interface such that $\Gamma(s, 0) = 1$. Unless otherwise, we set the Reynolds number $Re = 10$, the capillary number $Ca = 0.5$, the surface Peclet number $Pe_s = 10$, and the parameter $\beta = 0.25$.

4.1. Convergence test of fluid velocity and surfactant concentration

Before we proceed, we first carry out the convergence study of the present method. Here, we perform different computations with varying Cartesian mesh $h = \Delta x = \Delta y = 0.04, 0.02, 0.01, 0.005$. The Lagrangian mesh is chosen as $\Delta s \approx h/2$ and the time step size is $\Delta t = h/8$. The solutions are computed up to time $T = 1$.

Since the analytical solution is not available in these simulations, we choose the results obtained from the finest mesh as our reference solution and compute the L_2 error between the reference solution and the solution obtained from the coarser grid. Table 1 shows the mesh refinement analysis of the velocity u, v, and the

Table 1
The mesh refinement analysis of the velocity u, v, and the surfactant concentration Γ

h	$\|u - u_{ref}\|_2$	Rate	$\|v - v_{ref}\|_2$	Rate	$\|\Gamma - \Gamma_{ref}\|_2$	Rate
0.04	4.9739E−03	–	4.1656E−03	–	1.4551E−02	–
0.02	2.1476E−03	1.21	1.8169E−03	1.20	6.3542E−03	1.20
0.01	6.9859E−04	1.62	6.2180E−04	1.55	2.2329E−03	1.51

surfactant concentration Γ. One can see that the error decreases substantially when the mesh is refined, and the rate of convergence is about 1.5. Notice that, the fluid variables are defined at the staggered grid and the surfactant concentration is defined at "half-integer" grid, so when we refine the mesh, the numerical solutions will not coincide with the same grid locations. In these runs, we simply use a linear interpolation to compute the solutions at the desired locations. We attribute this is part of the reason why the rate of convergence behaves less than second-order.

4.2. Clean vs. contaminated interface

To examine the effect of the surfactant on interfacial dynamics, we compare a drop with and without surfactant in a steady shear flow. When the surfactant are present in the interface, the surface tension can be reduced significantly, cf. equation of state (13). Throughout the rest of this paper, we use a uniform Cartesian mesh $h = \Delta x = \Delta y = 0.02$, and a Lagrangian grid with size $\Delta s \approx h/2$. The time step size is set to be $\Delta t = h/8$.

Fig. 1 shows the time evolution plots of drop deformation in a steady shear flow field. Here, we consider three different values of β in Eq. (13); namely, $\beta = 0$ (dotted, clean interface), $\beta = 0.25$ (dash-dotted), and $\beta = 0.5$ (solid). As expected, the magnitude of drop deformation increases when the value of β increases, as in the case of Stokes flow [25]. Fig. 2 shows the vorticity plot for the drop with surfactant near the left and the right tips. One can see that two vortices with positive and negative signs are generated near the drop tips.

During the drop deformation, the Lagrangian markers will gradually sweep into the tips and cause clustered distribution near the tips. If the markers become too crowdedly or too coarsely distributed, it will affect the numerical accuracy. Thus, in order to maintain the numerical stability and accuracy, we need to perform grid redistribution if necessary. The detail is given as follows.

In each time step, we compute the distance between two adjacent markers. If the distance is within an interval $[0.25h, h]$, then we basically keep the original resolution. However, if the distance is smaller than $0.25h$, then we remove some of the markers. Similarly, when the distance is larger than h, we add more points between these two markers. In general, we just keep the distance between two adjacent markers in a reasonable range. One important thing during the grid redistribution process is to keep the mass conservation of the surfactant. This can be done in a local way. For instance, in the segment of adding more grid points, we simply
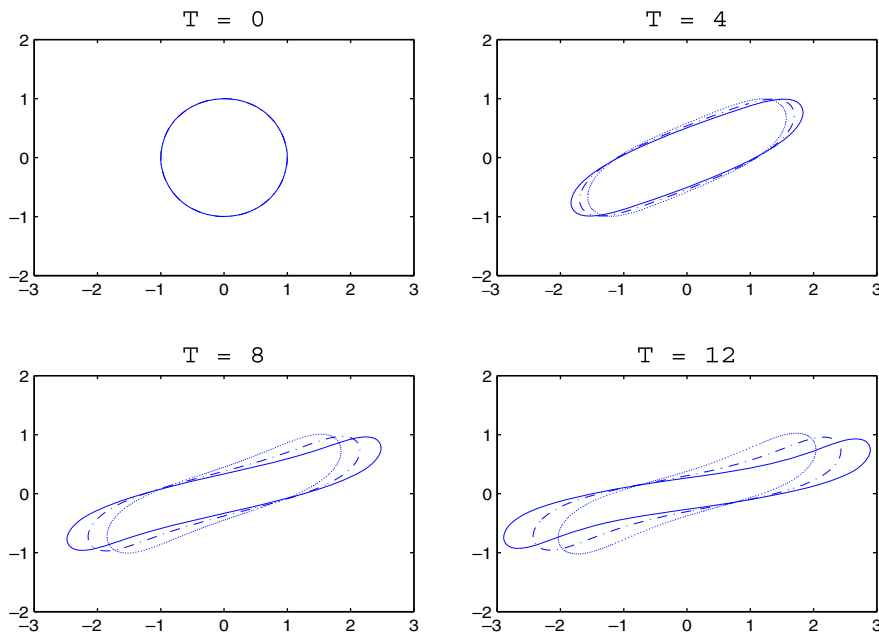
Fig. 1. The time evolution of a drop in a shear flow with clean ($\beta = 0$, '·····') and contaminated interface ($\beta = 0.25$, '–·–·–·–', $\beta = 0.5$, '———').
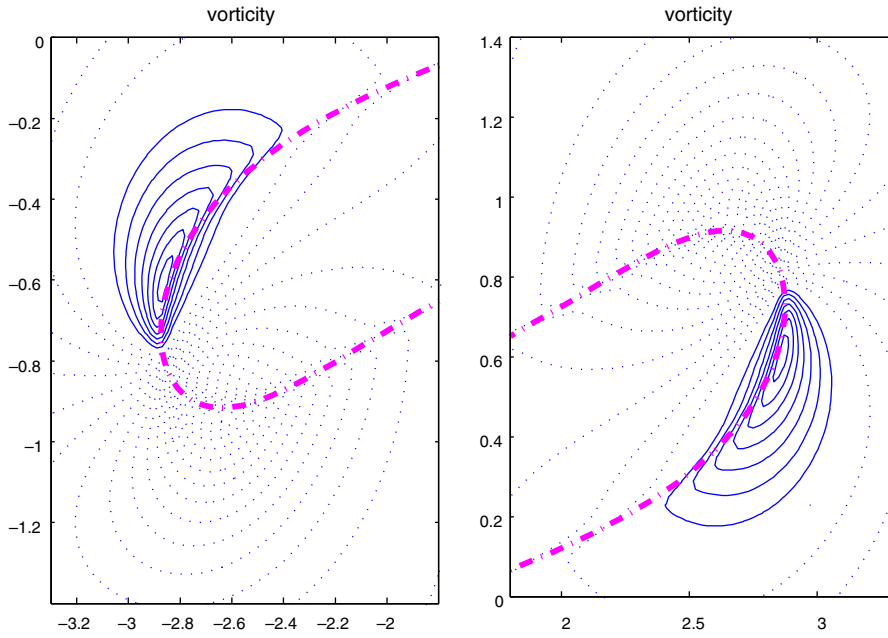
Fig. 2. The vorticity plot for the drop with surfactant near the left and right tips ($\beta = 0.5, T = 12$).

distribute the surfactant mass into those points uniformly. On the other hand, in the segment of removing grid points, we add up those surfactant mass to be a new surfactant concentration in the new combining segment. Thus, the overall surfactant mass is conserved exactly without any scaling.

Plots of the corresponding surfactant concentration (left column) and surface tension (right column) vs. arc-length are given in Fig. 3. For the surfactant concentration plot, we omit the case of clean interface since
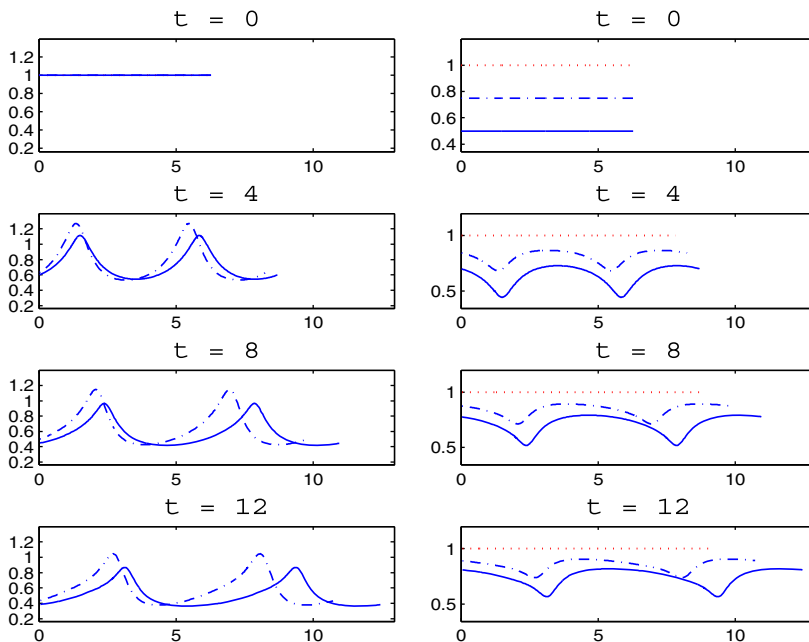
Fig. 3. Distributions of the surfactant concentration (left) and the corresponding surface tension (right). Notations and parameters are same as in Fig. 1.

the concentration is zero everywhere on the interface. It can be seen from this figure, the drop is elongated by the shear flow so that the total length of the interface is increased from the rest state. Since there is no surfactant transferred between the interface and the fluid, the surfactant concentration is diluted on a portion of the interface, partly due to the elongation of the interface, but mainly because it is swept to the drop tips. As a result, the smallest surface tension occurs at the drop tips. One can also see that the value of β affects the surfactant concentration by shifting the distributions slightly along the drop length. Once again, we confirm the same qualitative behavior as in [25].

In Fig. 4, the corresponding capillary (defined as $\sigma\kappa|\frac{\partial X}{\partial s}|/(ReCa)$, left column) and the Marangoni forces (defined as $\frac{\partial\sigma}{\partial s}/(ReCa)$, right column) are plotted vs. the arc-length for different cases of β. Since the capillary force depends on the curvature and surface tension, we see that the largest capillary force occurs at the drop tips due to the high curvature there. For clean interface, the Marangoni force is obviously zero.

In Fig. 5, we present four different plots: namely, (a) total mass of the surfactant; (b) the error of total mass, $m(t) - m(0)$; (c) total area of the drop; (d) total length of the drop interface. Clearly, the present method preserves the total surfactant mass and the errors reach machine precision. However, there is a slight area losing or fluid leakage in the drop as shown in Fig. 5c. It seems that the drop without surfactant has a more serious leakage than the ones with surfactant. It is well-known that the fluid leakage often appears in the simulation of immersed boundary method. In [16], Peskin and Printz proposed an improved volume (area in 2D) conservation scheme for the immersed boundary method by constructing a discrete divergence operator based on the interpolation scheme. Here, however, the area loss is not that significant, thus no modification is applied. Once again, we can see from Fig. 5d that the drop with surfactant has larger deformation than the one without surfactant due to the increase of total length of the interface.

4.3. Linear vs. nonlinear equation of state

In this test, we use the same set up as in the previous one except that a simplified form of nonlinear Langmuir equation of state $\sigma(\Gamma) = \sigma_c(1 + \ln(1 - \beta\Gamma))$ is used and compared with the results of the linear equation of the state. In Fig. 6, the evolution of the drop under steady shear flow is shown at different times using the linear (dotted) and nonlinear (solid) equations of state with $\beta = 0.5$. Once again, our results are consistent
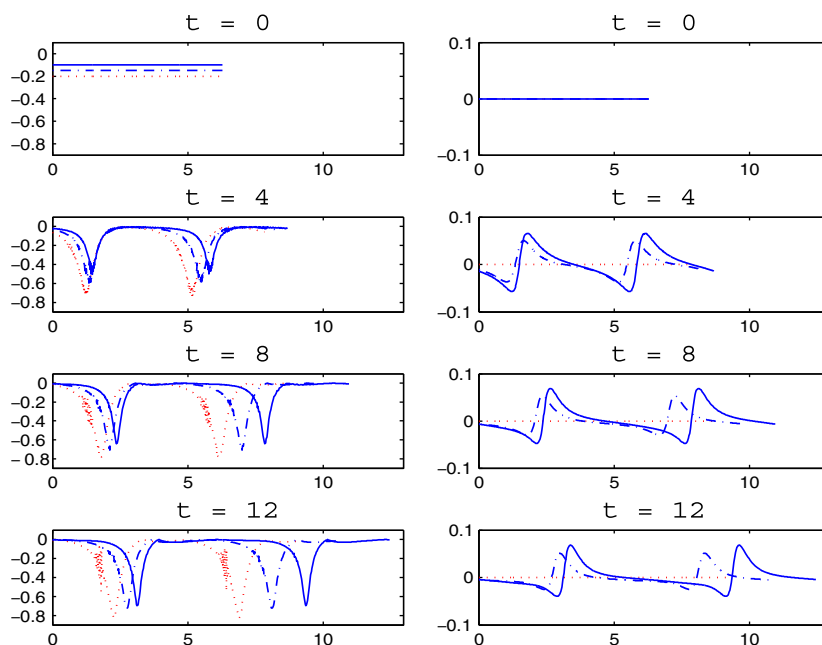
Fig. 4. The corresponding capillary force (left) and Marangoni force (right). Notations and parameters are same as in Fig. 1.
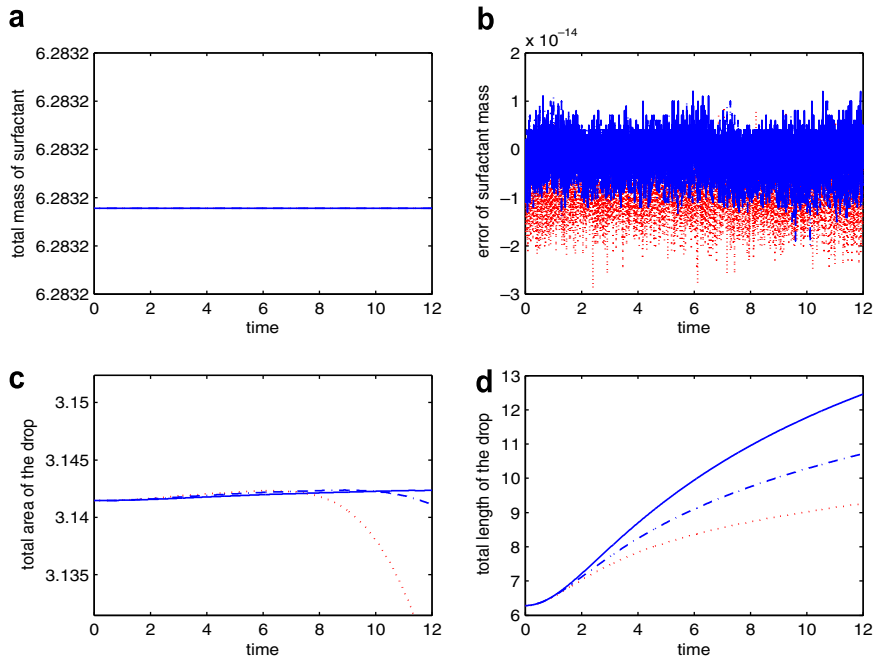
Fig. 5. (a) Total mass of the surfactant. (b) Time plot of $m(t) - m(0)$. (c) Total area of the drop. (d) Total length of the drop interface. Notations and parameters are same as in Fig. 1.
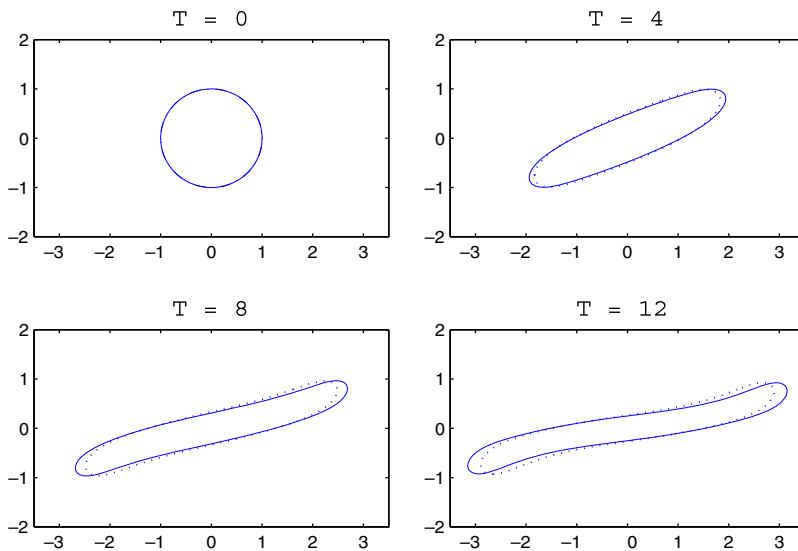
Fig. 6. The time evolution of a drop under a shear flow with linear ('····') and nonlinear ('——') equation of state.

with those in [25], i.e., drop deformation increases when the nonlinear equation of state is used. The corresponding surfactant concentrations and surface tensions are shown in Fig. 7. One can easily see that the nonlinear equation of state generates smaller surface tension at drop tips which leads to a larger deformation. As shown in Fig. 8, the capillary forces are roughly similar but the Marangoni force for the nonlinear case is slightly larger at the drop tips. The four different plots for both linear and nonlinear cases including the total mass of the surfactant, the error of total mass, the total area of the drop, and the total length of the drop are shown in Fig. 9.
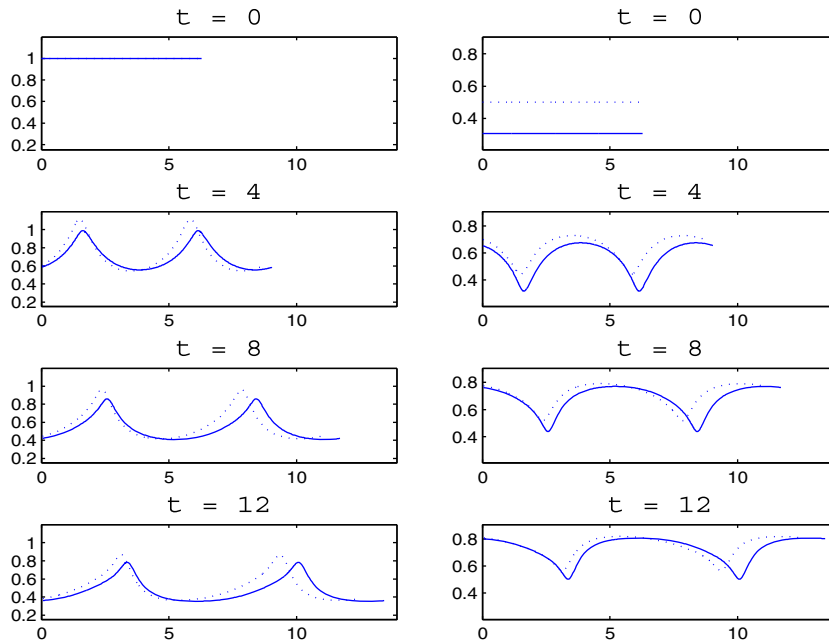
Fig. 7. Distributions of the surfactant concentration (left) and the corresponding surface tension (right). Notations and parameters are same as in Fig. 6.
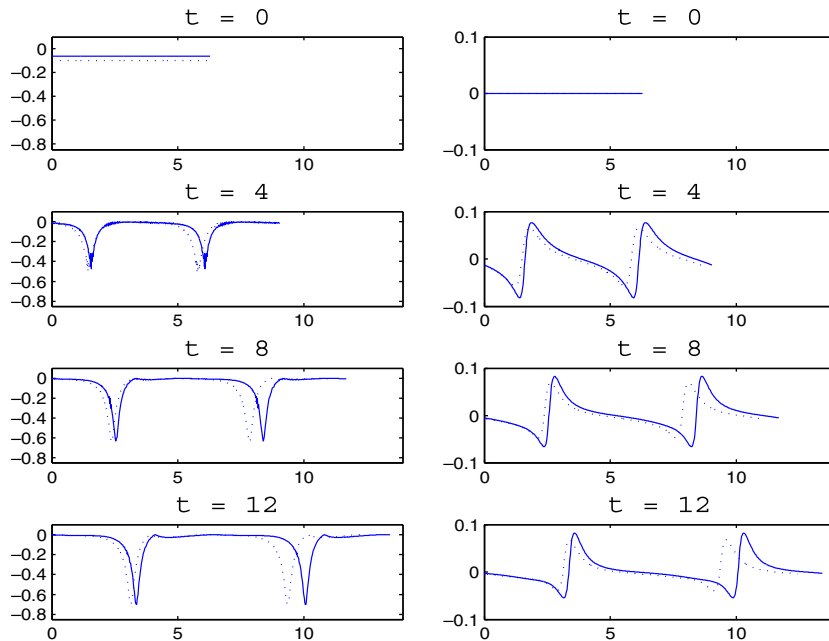
Fig. 8. The corresponding capillary force (left) and Marangoni force (right). Notations and parameters are same as in Fig. 6.

4.4. Effect of capillary number on drop deformation

As the last test, we perform the study on how different capillary numbers affect the drop deformation. Here, we fix the Reynolds number $Re = 10$ and the surface Peclet number $Pe_s = 10$. We vary the capillary number as
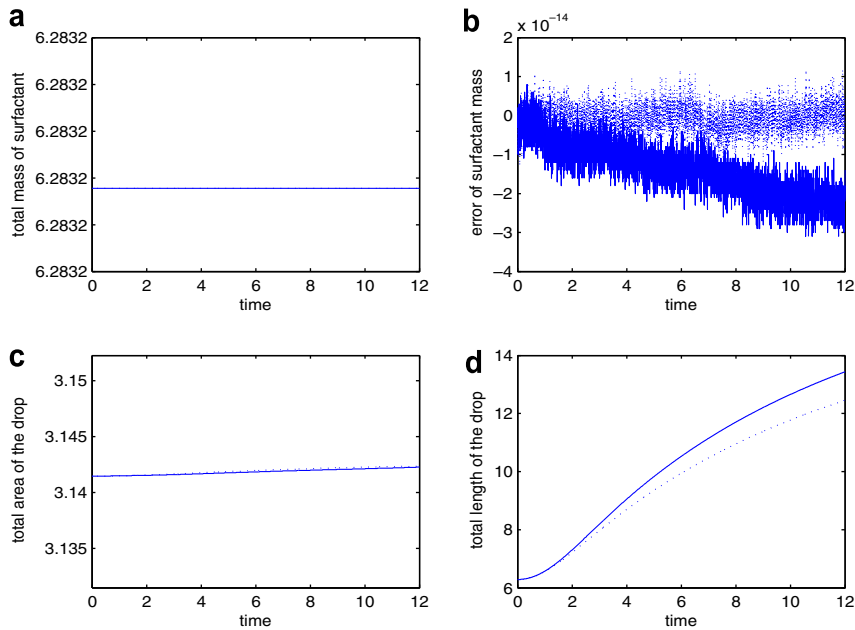
Fig. 9. (a) Total mass of the surfactant. (b) Time plot of $m(t) - m(0)$. (c) Total area of the drop. (d) Total length of the drop interface. Notations and parameters are same as in Fig. 6.
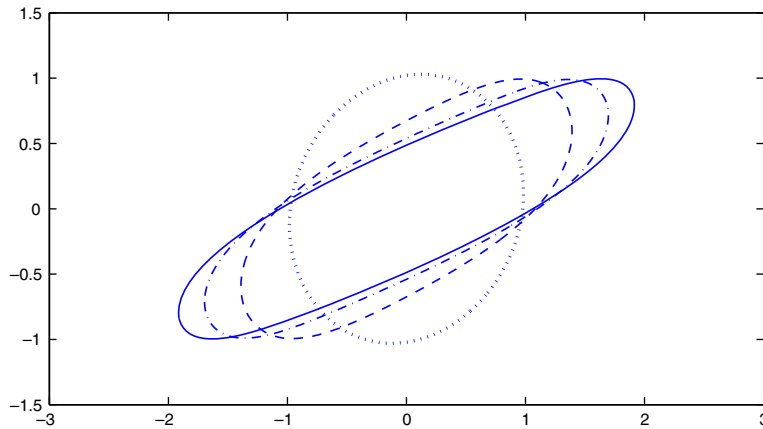
Fig. 10. The effect of capillary number Ca on the drop deformation ($Ca = 0.05$: '⋯⋯', $Ca = 0.25$: '– – – –', $Ca = 0.5$: '⋅– ⋅⋅ – ⋅', $Ca = 1.0$: '——').

$Ca = 0.05, 0.25, 0.5, 1.0$ and perform our runs up to time $T = 4$. As confirmed in previous literature such as [12], a larger capillary number means a smaller surface tension (with the viscosity fixed) so the drop under shear flow can deform more substantially. This is exactly what we see in our simulation as illustrated in Fig. 10. We also make runs by varying the different surface Peclet number while keeping the Reynolds and capillary numbers fixed. However, the effect of surface Peclet number is not as significant as the effect of the capillary number on drop deformations, so we omit the results here.

5. Conclusion

In this paper, we have developed an immersed boundary method for two-dimensional fluid interfacial problems with insoluble surfactant. The governing equations are formulated in a usual immersed boundary frame-

work where a mixture of Eulerian fluid and Lagrangian interfacial variables are used, with the linkage between those two different variables is provided by Dirac delta function. The immersed boundary force comes from the surface tension which is affected by the distribution of surfactant along the interface. By tracking the interface in a Lagrangian manner, a simplified surfactant concentration equation can be obtained. The numerical method involves solving the Navier–Stokes equations on a staggered grid by a semi-implicit pressure increment projection method where the immersed interfacial forces are calculated at the beginning of each time step. Once the velocity values and interfacial configurations are obtained, a new symmetric discretization for the surfactant concentration equation is used such that the total mass of surfactant is conserved numerically.

As a next step, we will generalize the present algorithm to simulate two phase flows with distinct densities and viscosities. In particular, we plan to study the effect of soluble surfactant on drop detachment from a solid surface, i.e., a problem with moving contact points/lines. Finally, we plan to generalize the current work to 3D simulations.

Acknowledgments

References

[1] J. Adams, P. Swarztrauber, R. Sweet, Fishpack – a package of Fortran subprograms for the solution of separable elliptic partial differential equations, 1980. <http://www.netlib.org/fishpack>.
[2] R. Aris, Vectors, Tensors, and the Basic Equations of Fluid Mechanics, Prentice-Hall, Englewood Cliffs, NJ, 1962.
[3] D.L. Brown, R. Cortez, M.L. Minion, Accurate projection methods for the incompressible Navier–Stokes equations, J. Comput. Phys. 168 (2001) 464–499.
[4] H.D. Ceniceros, The effects of surfactants on the formation and evolution of capillary waves, Phys. Fluids 15 (1) (2003) 245–256.
[5] P.G. De Gennes, F. Brochard, D. Quere, Gouttes, Bulles, Perles Ondes, Edition Berlin, 2002.
[6] F.H. Harlow, J.E. Welsh, Numerical calculation of time-dependent viscous incompressible flow of fluid with a free surface, Phys. Fluids 8 (1965) 2181–2189.
[7] H. Huang, M.-C. Lai, H.-C. Tseng, A parametric derivation of the surfactant transport equation along a deforming fluid interface, submitted for publication.
[8] M. Hameed, M. Siegel, Y.-N. Young, J. Li, M.R. Booty, D.T. Papageorgiou, Influence of insoluble surfactant on the deformation and breakup of a bubble or thread in a viscous fluid, J. Fluid Mech. 594 (2008) 307–340.
[9] A.J. James, J.S. Lowengrub, A surfactant-conserving volume-of-fluid method for interfacial flows with insoluble surfactant, J. Comput. Phys. 201 (2004) 685–722.
[10] L.D. Landau, E.M. Lifshitz, Fluid Mechanics, Pergamon Press, New York, 1958.
[11] R. LeVeque, Z. Li, The immersed interface method for elliptic equations with discontinuous coefficients and singular sources, SIAM J. Numer. Anal. 31 (1994) 1019–1044.
[12] J. Lee, C. Pozrikidis, Effect of surfactants on the deformation of drops and bubbles in Navier–Stokes flow, Comput. Fluids 35 (2006) 43–60.
[13] M. Muradoglu, G. Tryggvason, A front-tracking method for computations of interfacial flows with soluble surfactants, J. Comput. Phys. 227 (2008) 2238–2262.
[14] C.S. Peskin, Flow patterns around heart valves: a numerical method, J. Comput. Phys. 10 (1972) 252.
[15] C.S. Peskin, The immersed boundary method, Acta Numerica 11 (2002) 1–39.
[16] C.S. Peskin, B.F. Printz, Improved volume conservation in the computation of flows with immersed elastic boundaries, J. Comput. Phys. 105 (1993) 33–36.
[17] Y. Pawar, K.J. Stebe, Marangoni effects on drop deformation in an extensional flow: the role of surfactant physical chemistry, I. Insoluble surfactants, Phys. Fluids 8 (1996) 1738.
[18] L.E. Scriven, Dynamics of a fluid interface, Chem. Eng. Sci. 12 (1960) 98.
[19] H.A. Stone, A simple derivation of the time-dependent convective–diffusion equation for surfactant transport along a deforming interface, Phys. Fluids A 2 (1) (1990) 111–112.
[20] P. Tabeling, Introduction to Microfluidics, Oxford University Press, 2005.
[21] G. Tryggvason, B. Bunner, A. Esmaeeli, D. Juric, N. Al-Rawahi, W. Tauber, J. Han, S. Nas, Y.-J. Jan, A front-tracking method for the computations of multiphase flow, J. Comput. Phys. 169 (2001) 708–759.

[22] S.O. Unverdi, G. Tryggvason, A front-tracking method for viscous incompressible multi-fluid flows, J. Comput. Phys. 100 (1992) 25–37.

[23] H. Wong, D. Rumschitzki, C. Maldarelli, On the surfactant mass balance at a deforming fluid interface, Phys. Fluids 8 (11) (1996) 3203–3204.

[24] A.M. Waxman, Dynamics of a couple-stress fluid membrane, Stud. Appl. Math. 70 (1984) 63.

[25] J.-J. Xu, Z. Li, J.S. Lowengrub, H.-K. Zhao, A level-set method for interfacial flows with surfactant, J. Comput. Phys. 212 (2006) 590–616.

[26] J.-J. Xu, H.-K. Zhao, An Eulerian formulation for solving partial differential equations along a moving interface, J. Sci. Comput. 19 (2003) 573–593.